19

Unified Power Flow Controllers Without Energy Storage: Designing Power Controllers for the Matrix Converter Solution

Joaquim Monteiro[1], J. Fernando Silva[2], Sónia Pinto[2] and João Palma[3]
[1]*Cie3 and ISEL – Polytechnic Institute of Lisbon,*
[2]*Cie3 and IST – Technical University of Lisbon,*
[3]*SIC – National Laboratory for Civil Engineering,*
Portugal

1. Introduction

In the last years the growing economic, environmental and social concerns have increased the difficulty to use fossil fuels, as well as to obtain new licenses to build either transmission lines (right-of-way) or high power facilities. This led to the continuous growth of decentralized electricity generation (using renewable energy resources) (Hingorani, 2000). This scenario has introduced new problems and technical challenges to power systems researchers and electricity markets participants. One of the main consequences of these changes has been the substantial increase of power transfer within transmission networks, approaching their rated capacity and requiring adequate control capability to supply the continuously growing demand of electric power.

To solve these issues Flexible AC Transmission Systems (FACTS) became a well known power electronics based solution to control power flow in transmission lines. These systems are switching controlled converters that operate in real time increasing the transmission lines power flow capacity up to their thermal limits. Currently, Unified Power Flow Controllers (UPFC) are the most versatile and complex FACTS enabling accurate and reliable control of both active and reactive power flow over networks, through load sharing between alternative line paths (Song et al , 1999).

The original UPFC concept was proposed by L. Gyugyi (Gyugyi, 1992), and consisted of the combination of a Static Synchronous Compensator (STATCOM) and a Static Synchronous Series Compensator (SSSC) connected by a common DC link, using large high-voltage DC storage capacitors. The AC converters sides of these compensators are connected to a transmission line, through coupling transformers, in shunt and series connection with the line. This arrangement operates as an ideal reversible AC-AC switching power converter allowing shunt and series compensation and bidirectional power flow, between the AC terminals of the two converters.

The DC capacitor bank used in the UPFC topology to link the two back-to-back converters increases the UPFC weight, cost, occupied area and introduces additional losses. Replacing the double three-phase inverter by one three phase matrix converter the DC link capacitors are eliminated, reducing costs, size, maintenance, and increasing reliability and lifetime. The

AC-AC matrix converter, also known as all silicon converter, processes the energy directly without large energy storage needs, allows bi-directional power flow, while it guarantees input and output sinusoidal voltages and currents with variable amplitude and frequency and adjustable power factor. On the other way, the matrix converter control is more complex than the control of the back-to-back converter.

Over the years the interesting properties presented by the matrix converter pushed the design of their controllers, so that matrix converters are being used quite successfully in many industrial applications, such as in power sources for electrical drives with variable speed (Matsuo et al, 1996), in applications related to power quality enhancement in the electrical grid (Galkin et al, 2001), in renewable power supply systems (Nikkhjoei et al, 2005) and also in the compensation of harmonics in power network as dynamic voltage restorers (DVR) (Wang et al, 2009).

In general, the conventional control methods of UPFCs are based on power systems linearized models, valid around an operating point. Usually, these linearized models do not guarantee robustness and insensitivity to the parameters and may give rise to poor dynamic response and/or undesired instability, since most of these controllers do not have the capacity to adapt to nonlinearities or continuously changing dynamics of the power system (Monteiro et al, 2005), (Liu et al, 2007). In addition, many of the control strategies used in the UPFC are based in proportional integral controllers obtained from its dynamic model in *dq* coordinates to improve performance and reduce the interaction between the control of active and reactive power (Round et al, 1996).

In this chapter, the use of a UPFC without energy storage, based on a matrix converter topology, is proposed to control the active and reactive power flow in the transmission line (section 2). Decoupled controllers (Verveckken et al, 2007) using the inverse dynamics linearization approach are proposed for active and reactive power control. These controllers allow the elimination of the cross-coupling effect between active and reactive power controllers and fast response (section 3). The designed controllers are implemented using digital signal processing (DSP) hardware together with a matrix converter prototype and laboratory equipment to emulate the power network (section 4). The dynamic and steady-state performance of the proposed power control methods are evaluated both by simulation and by experimental results (section 5). Finally, conclusions are listed regarding the behaviour of the overall matrix converter based UPFC when operated with the proposed active and reactive power controllers (section 6).

2. Modelling of UPFC power system

A simplified power transmission network using the proposed matrix converter based UPFC is presented in Fig. 1. In this scheme V_S and V_R are, respectively, the sending-end and receiving-end sinusoidal voltages of the G_S and G_R generators feeding load Z_L consisting of a resistance R_L and an inductance L_L. The matrix converter is connected to transmission line 2, represented as a series inductance and resistance (L_{L2}, R_{L2}), through coupling transformers, T_1 in the shunt side and T_2 in the series side.

A detailed diagram of the UPFC system showing the connection of the matrix converter to the transmission line, in Fig. 2, includes three-phase shunt input transformer (T_a, T_b, T_c), three-phase series output transformer (T_A, T_B, T_C) and a three-phase matrix converter. In this diagram, the three-phase *LCr* input low pass filter is required to re-establish a voltage–source boundary to the matrix converter, also enabling smooth input currents.

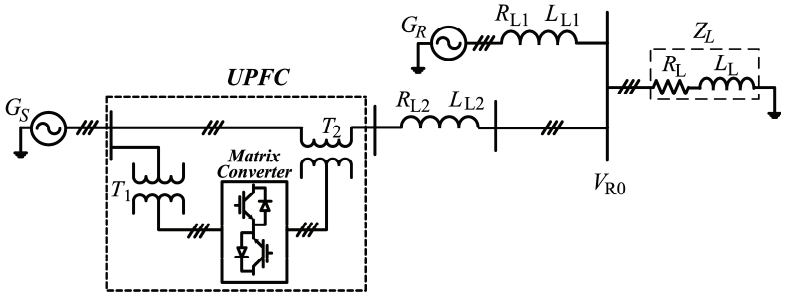

Fig. 1. A transmission network with a matrix converter UPFC.

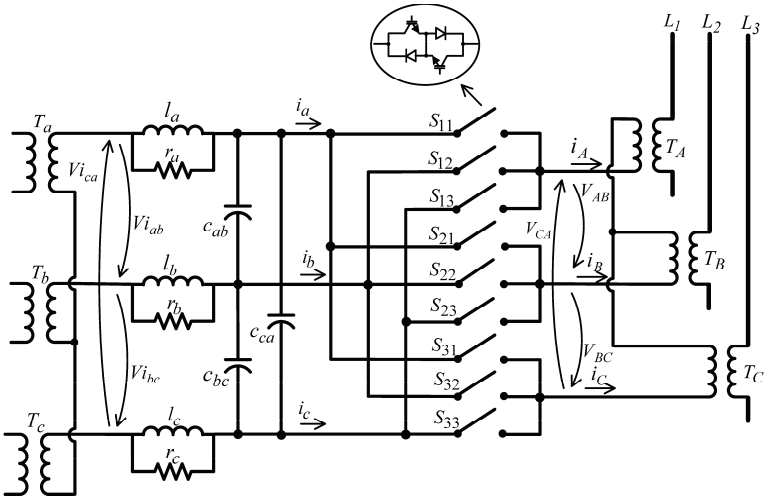

Fig. 2. Detailed matrix converter based UPFC.

The next subsections will detail the matrix converter and the UPFC dynamic model.

2.1 Matrix converter model

The matrix converter UPFC system (Fig. 2) modelling assumes ideal voltage sources and ideal shunt and series transformers. Considering also ideal power semiconductors, each matrix converter bi-directional switch S_{kj} (k, $j \in \{1,2,3\}$) can only have two possible states: "S_{kj}=1" if the switch is closed or "S_{kj}=0" if the switch is open. The nine switches of the matrix converter can be represented as a 3x3 matrix (1):

$$S = \begin{bmatrix} S_{11} & S_{12} & S_{13} \\ S_{21} & S_{22} & S_{23} \\ S_{31} & S_{32} & S_{33} \end{bmatrix} \tag{1}$$

The matrix converter topological constraints imply that $\sum_{j=1}^{3} S_{kj} = 1$, for all $k \in \{1,2,3\}$.

According to (1), the relationship between load and input voltages can be expressed as:

$$\begin{bmatrix} v_A & v_B & v_C \end{bmatrix}^T = S \begin{bmatrix} v_a & v_b & v_c \end{bmatrix}^T \tag{2}$$

Using the transpose of matrix S, the input phase currents can be related to the output phase currents, by (3).

$$\begin{bmatrix} i_a & i_b & i_c \end{bmatrix}^T = S^T \begin{bmatrix} i_A & i_B & i_C \end{bmatrix}^T \tag{3}$$

From the 27 possible switching patterns ($_3^3$), time variant vectors can be obtained (Pinto et al, 2001), representing the output voltages and input currents in $\alpha\beta$ coordinates.
The command of the matrix converter switches can be accomplished using a Venturini based high frequency PWM modulator (Alesina et al, 1981) , (Wheeler, 2002) (4).

$$\begin{aligned} m_{kj}(t) = 1/3 + (1/3)\Big\{ & \left(v_k v_j\right) \Big/ V_i^2 + \\ & + \left(4/3\sqrt{3}\right) q\, sen\left(\omega_i t - \beta_k\right) sen\left(3\omega_i t\right) \Big\} \end{aligned} \tag{4}$$

$$k = a, b, c;\ \ j = A, B, C;\ \ q = V_o / V_i;\ \ \beta_k = 0, 2\pi/3, 4\pi/3$$

This PWM method yields near sinusoidal output voltages with amplitude defined by an active power controller and phase defined by a reactive power controller, as well as almost sinusoidal input currents with near unity input power factor, if needed.

2.2 UPFC dynamic model

The scheme presented in Fig. 3 shows the simplified three-phase equivalent circuit of matrix UPFC transmission system model. For dynamic system modelling, the power sources and the coupling transformers are all considered ideal, including the matrix converter represented as a controllable voltage source, with amplitude V_C and phase ρ.
In this circuit L_2 and R_2 are, respectively, the Thévenin equivalent inductance and resistance calculated by: $L_2 = L_{L2} + L_{L1} // L_L$ and $R_2 = R_{L2} + R_{L1} // R_L$. Besides, V_{R0} is the voltage at the load bus.

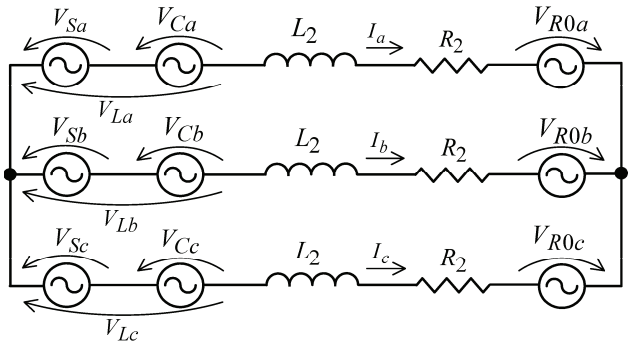

Fig. 3. Three phase equivalent circuit of matrix UPFC and transmission line.

Considering a symmetrical and balanced three phase system and applying Kirchhoff laws to the three phase equivalent circuit in Fig. 3, the dynamic equations of AC line currents are obtained in *dq* coordinates as follows:

$$\frac{dI_d}{dt} = \omega I_q - \frac{R_2}{L_2} I_d + \frac{1}{L_2}\left(V_{Ld} - V_{R0d}\right) \tag{5}$$

$$\frac{dI_q}{dt} = -\omega I_d - \frac{R_2}{L_2} I_q + \frac{1}{L_2}\left(V_{Lq} - V_{R0q}\right) \tag{6}$$

In the last equations, V_{Ld} and V_{Lq} are introduced for notation simplicity and are given by: $V_{Ld}=V_{Sd}+V_{Cd}$ and $V_{Lq}=V_{Sq}+V_{Cq}$.
Applying Laplace transform to system transfer functions (5) and (6), equation (7) is obtained:

$$\left(s + \frac{R_2}{L_2}\right)\begin{bmatrix} I_d \\ I_q \end{bmatrix} = \omega\begin{bmatrix} I_q \\ -I_d \end{bmatrix} + \frac{1}{L_2}\begin{bmatrix} V_{Ld} - V_{R0d} \\ V_{Lq} - V_{R0q} \end{bmatrix} \tag{7}$$

Solving (7) in order to the line currents I_d I_q, equation (8) may be obtained as a function of voltages V_{Ld}, V_{Lq} and V_{R0d}, V_{R0q} at the receiving end.

$$\begin{bmatrix} I_d \\ I_q \end{bmatrix} = \frac{\frac{1}{L_2}\begin{bmatrix} s + \frac{R_2}{L_2} & \omega \\ -\omega & s + \frac{R_2}{L_2} \end{bmatrix}}{\left(s + \frac{R_2}{L_2}\right)^2 + \omega^2}\begin{bmatrix} V_{Ld} - V_{R0d} \\ V_{Lq} - V_{R0q} \end{bmatrix} \tag{8}$$

Active and reactive powers of sending end generator are given in *dq* coordinates by (9):

$$\begin{bmatrix} P \\ Q \end{bmatrix} = \begin{bmatrix} V_{Sd} & V_{Sq} \\ V_{Sq} & -V_{Sd} \end{bmatrix}\begin{bmatrix} I_d \\ I_q \end{bmatrix} \tag{9}$$

The active and reactive power controllers will be designed based on the previous equations.

3. Designing active and reactive power controllers

In this chapter, new linear controllers will be derived in *dq* coordinates to guarantee no cross-coupling between active and reactive power controllers and fast response, using inverse dynamics linearization. The synthesis of these controllers is also based on a modified Venturini high frequency modulator.

3.1 Matrix converter UPFC controllers design by inverse dynamics linearization

The dynamic equations of UPFC model (8) show that there is no dynamics related to the power sources voltages, which are considered ideal. So in *dq* Laplace domain the power

sources voltages are constant. Assuming both V_{ROd} and V_{Sd} as constant and a rotating reference frame synchronized to the V_S source so that $V_{Sq}=0$, active and reactive power P and Q will be obtained by (10) and (11).

$$P = V_{Sd} I_d \tag{10}$$

$$Q = -V_{Sd} I_q \tag{11}$$

The synthesis of active and reactive power controllers is obtained substituting the previously calculated currents in dq coordinates (8) on (10) and (11). Active and reactive powers are obtained as a function of transmission line parameters, load bus and sources voltages.

$$\begin{aligned} P = V_{Sd} & \frac{(sL_2 + R_2)(V_{Sd} - V_{R0d}) - \omega L_2 V_{R0q}}{(sL_2 + R_2)^2 + (\omega L_2)^2} \\ & + V_{Sd} \frac{(sL_2 + R_2) V_{Cd} + \omega L_2 V_{Cq}}{(sL_2 + R_2)^2 + (\omega L_2)^2} \end{aligned} \tag{12}$$

$$\begin{aligned} Q = V_{Sd} & \frac{(sL_2 + R_2) V_{R0q} + \omega L_2 (V_{Sd} - V_{R0d})}{(sL_2 + R_2)^2 + (\omega L_2)^2} \\ & + V_{Sd} \frac{\omega L_2 V_{Cd} - (sL_2 + R_2) V_{Cq}}{(sL_2 + R_2)^2 + (\omega L_2)^2} \end{aligned} \tag{13}$$

Both active and reactive powers, obtained respectively by equations (12) and (13), consist of an uncontrollable constant part (P_i, Q_i) based on sending end power source voltages and line impedance, and a controllable dynamic part (ΔP, ΔQ) determined by the matrix converter voltages. These relationships are presented in (14) and (15).

$$P = P_i + \Delta P \tag{14}$$

$$Q = Q_i + \Delta Q \tag{15}$$

From (12) and (13), the controllable part of steady-state active and reactive power (ΔP, ΔQ) can be obtained expressed as a function of matrix converter voltages in dq coordinates according to (16).

$$\begin{bmatrix} \Delta P \\ \Delta Q \end{bmatrix} = \frac{V_{Sd}}{(sL_2 + R_2)^2 + (\omega L_2)^2} \begin{bmatrix} sL_2 + R_2 & \omega L_2 \\ \omega L_2 & -(sL_2 + R_2) \end{bmatrix} \cdot \begin{bmatrix} V_{Cd} \\ V_{Cq} \end{bmatrix} \tag{16}$$

The controllable part of the active and reactive power flow components (16) may be written as in (17), introducing a matrix G_C for notation simplicity.

$$\begin{bmatrix} \Delta P \\ \Delta Q \end{bmatrix} = -\frac{V_{Sd}}{\det[G_C]} G_C \begin{bmatrix} V_{Cd} \\ V_{Cq} \end{bmatrix} \tag{17}$$

In (17) matrix G_C depends on the transmission line parameters (18) and its determinant is $\det[G_C] = -(sL_2 + R_2)^2 - (\omega L_2)^2$.

$$G_C = \begin{bmatrix} sL_2 + R_2 & \omega L_2 \\ \omega L_2 & -(sL_2 + R_2) \end{bmatrix} \tag{18}$$

The next section will present the controllers design based on the inverse dynamics linearization of the power system model.

3.2 Inverse dynamic linearization of the power system model

The proposed power controllers design use the inverse model of the power system to linearize and decouple active and reactive power control, calculating the control signals V_{Cd} and V_{Cq} as a function of the active and reactive power flow components ΔP, ΔQ. Knowing that $G_C = -(\det[G_C]).G_C^{-1}$, equation (19) is obtained.

$$\begin{bmatrix} V_{Cd} \\ V_{Cq} \end{bmatrix} = \frac{1}{V_{Sd}} G_C \begin{bmatrix} \Delta P \\ \Delta Q \end{bmatrix} \tag{19}$$

Considering a feedback loop controller topology for the power components, using the inverse system model (19) to design the controllers, and adding a linear integral controller to obtain zero static error, two decoupled equivalent systems with a first order system behavior with time constant T_P (being $[\Delta P \ \Delta Q]^T = 1/(sT_P+1)[\Delta P_{ref} \ \Delta Q_{ref}]^T$ can be obtained using (20).

$$\begin{bmatrix} \Delta P \\ \Delta Q \end{bmatrix} = \frac{1}{sT_p} \begin{bmatrix} \Delta P_{ref} - \Delta P \\ \Delta Q_{ref} - \Delta Q \end{bmatrix} \tag{20}$$

Multiplying both members of equation (20) by G_C/V_{Sd} control variables V_{Cd} and V_{Cq} are then obtained in (21) as independent functions of the active and reactive power errors, respectively.

$$\begin{bmatrix} V_{Cd} \\ V_{Cq} \end{bmatrix} = \frac{G_C}{V_{Sd}} \frac{1}{sT_p} \begin{bmatrix} \Delta P_{ref} - \Delta P \\ \Delta Q_{ref} - \Delta Q \end{bmatrix} \tag{21}$$

Based on the previous equations, the block diagram of Fig. 4 is obtained, representing the closed loop control system with decoupled active and reactive powers.

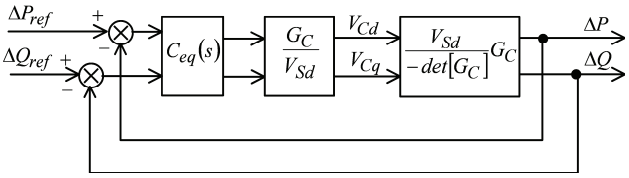

Fig. 4. Block diagram in closed loop control with active and reactive power decoupling.

Substituting in (21) the matrix G_C, an overall control system with decoupled controllers for active and reactive power is obtained (22).

$$\begin{bmatrix} V_{Cd} \\ V_{Cq} \end{bmatrix} = \frac{1}{V_{Sd}} \begin{bmatrix} \frac{sL_2 + R_2}{sT_p} & \frac{\omega L_2}{sT_p} \\ \frac{\omega L_2}{sT_p} & -\frac{sL_2 + R_2}{sT_p} \end{bmatrix} \begin{bmatrix} \Delta P_{ref} - \Delta P \\ \Delta Q_{ref} - \Delta Q \end{bmatrix} \tag{22}$$

The overall block diagram of the active and reactive power closed loop controllers, shown in Fig. 5, uses proportional integral controllers and integrators to generate the control variables (V_{Cd}, V_{Cq}) applied to the matrix converter modulator.

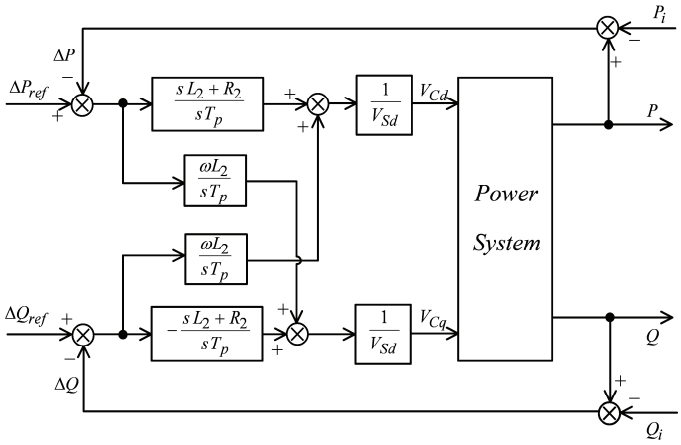

Fig. 5. The overall block diagram in closed loop control with controllers and power system.

This global diagram has also a power system block representing the sending end and receiving end voltage sources, the transmission lines, a three phase load and a three phase matrix converter connected to the transmission line through series and parallel power transformers.

4. Implementation of the power controllers

The implementation scheme of the active and reactive power controllers is shown on Fig. 6. This diagram presents the voltage sources (V_S and V_R) the transmission lines with resistance and inductance, an inductive three phase load and a three phase matrix converter connected to the line through power transformers (T_1, T_2). A digital signal processing (DSP) was used to implement the designed linear controllers for matrix vector selection at successive time steps.
To achieve safe commutation between matrix converter bidirectional switches, the four-step output current strategy was used (Huber et al, 1992). This commutation process was implemented in a field programmable gate array (FPGA) included in Fig. 6.
As shown in the previous diagram, the control of the instantaneous active and reactive power componets requires the measurement of G_S voltages, input currents and output currents, allowing the compensation of the active and reactive power errors, in real time.

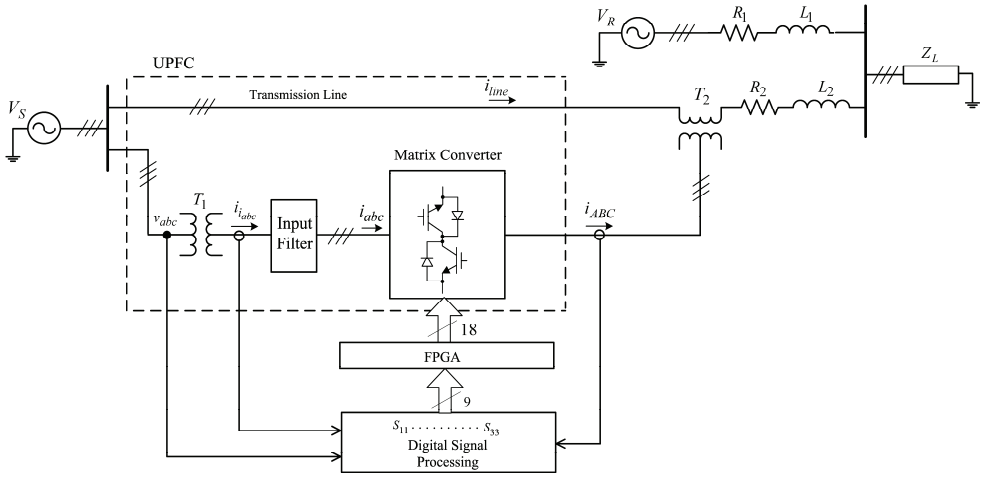

Fig. 6. Control scheme for the proposed method of a matrix converter operating as UPFC.

Based on this approach, at each time step the control system chooses the most suitable matrix vector upon the available set of discrete values corresponding to the set of acceptable switching states of all power semiconductors of the matrix converter.

5. Simulation and experimental results

In this section the dynamic and steady-state performance of the proposed active and reactive power control method is evaluated and discussed using detailed simulations and experimental implementation. A detailed simulation model representing matrix converter, series and shunt transformers, sources, transmission lines and additional blocks to simulate the control system is designed using MATLAB/Simulink and SimPowerSystems, being the matrix converter semiconductors represented as ideal switches.

Simulations are experimentally validated using a 3 kW prototype matrix converter, built with integrated power semiconductor modules, each one with six 1200V, 25A insulted gate bipolar transistors (IGBT) with anti-parallel diode in a common collector arrangement. The IGBT gates are driven by optically isolated drives (TLP250). The matrix converter input second order filter uses $l = 4.2\ mH$, $C = 6.6\ \mu F$, $r = 25\ \Omega$.

This prototype was connected to the laboratory low voltage network operating as UPFC (Fig. 6) with an input phase-to-phase matrix converter voltage equal to 120 V_{RMS}. Load power is 1.5 kW and the transmission lines 1 and 2 are emulated by inductances $L_1 = 12\ mH$, $L_2 = 15\ mH$ and series resistances $R_1 = R_2 = 0.2\ \Omega$, respectively, for lines 1 and 2. Current and voltage sensors were used respectively to measure matrix input and output currents (LEM LA25NP) and to measure the power network phase to phase voltages (LEM LV 25-P). Designed controllers were implemented using a DSP PowerPC board (dSPACE) and a FPGA from Xillinx for driving the commutation process.

Experimental and simulation results for the active and reactive power UPFC controllers using the proposed control method based in the linearized inverse dynamics were sized using time constant T_p=0.1ms, and T_s approximately equal to 23 μs.

Fig. 7 shows simulation (a) and experimental (b) results for the proposed controllers considering active and reactive power step response ($\Delta P_{ref} = +0.4\ pu$, $\Delta Q_{ref} = +0.2\ pu$) and initial reference values: P_{ref} =0.4 *pu*, Q_{ref} =0.2 *pu*. Results show decoupled active and reactive powers, fast response and a small ripple in steady state.

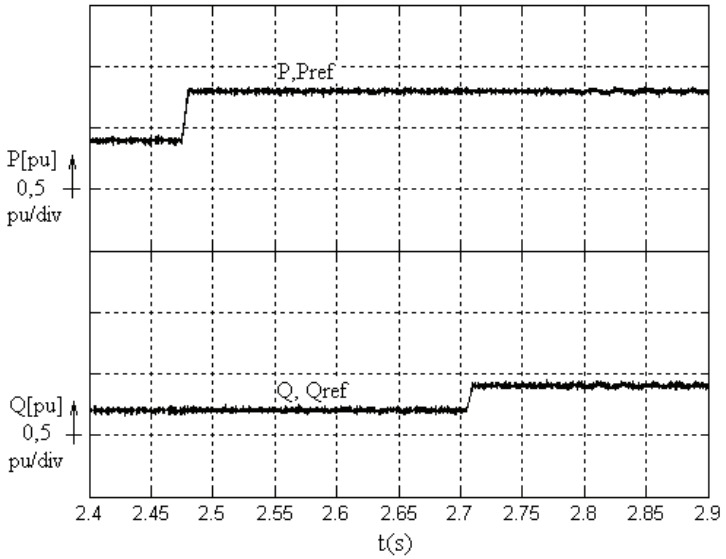

a)

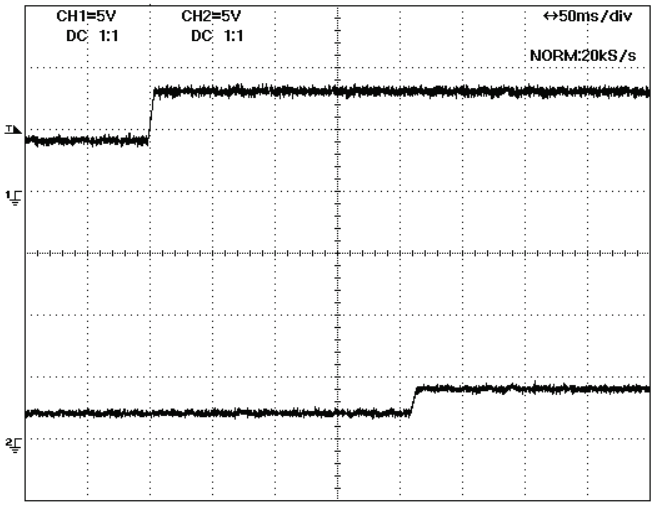

b)

Fig. 7. Active and reactive power response for a P and Q step when $\Delta P_{ref} = +0.4\ pu$ and $\Delta Q_{ref} = +0.2\ pu$. a) Simulation results. b) Experimental results.

Simulation and experimental results of Fig 8 show steady-state line and matrix converter input currents using the controllers proposed for P_{ref} =0.4 *pu*, Q_{ref} =0.2 *pu*. The results show that currents are almost sinusoidal with small ripple content.

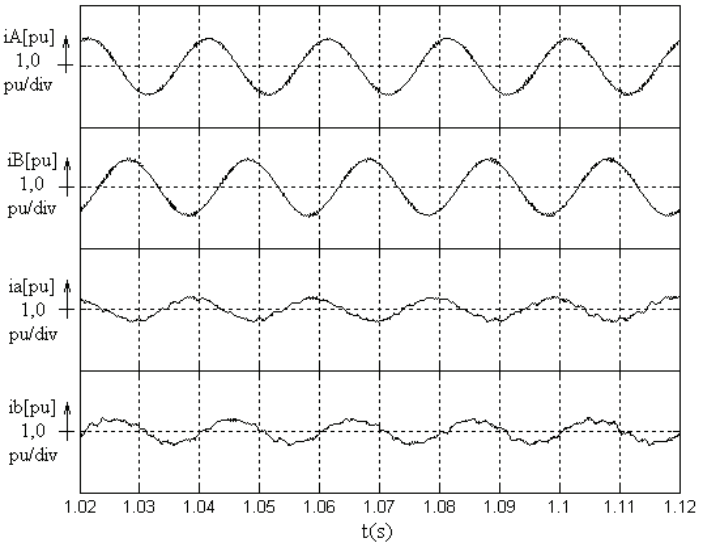

a)

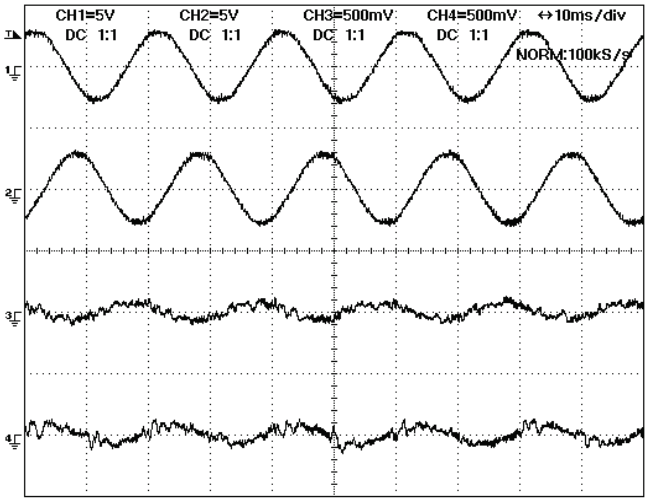

b)

Fig. 8. Line currents (i_A, i_B) and input matrix converter currents (i_b, i_c) for $P_{ref} = 0.4\ pu$ and $Q_{ref} = 0.2\ pu$. a) Simulation results. b) Experimental results.

The experimental power spectral density of transmission line and matrix converter current for the proposed controllers, in Fig. 9, shows that the main harmonics are nearly 33 dB below the 50Hz fundamental for the line current, and 20 dB below the 50Hz fundamental for the matrix converter current.

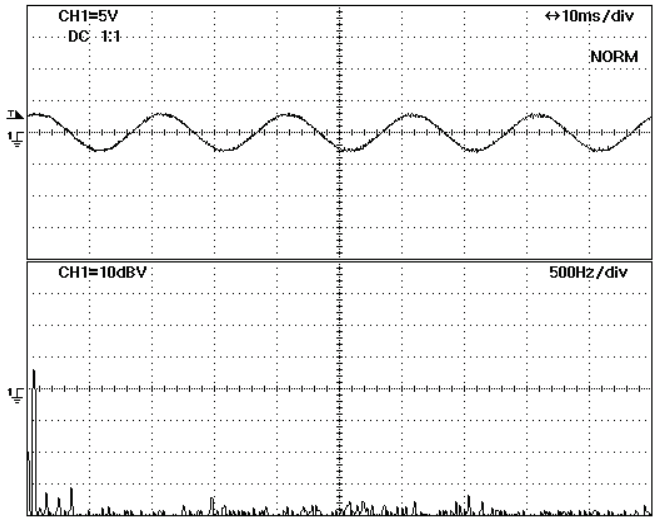

a)

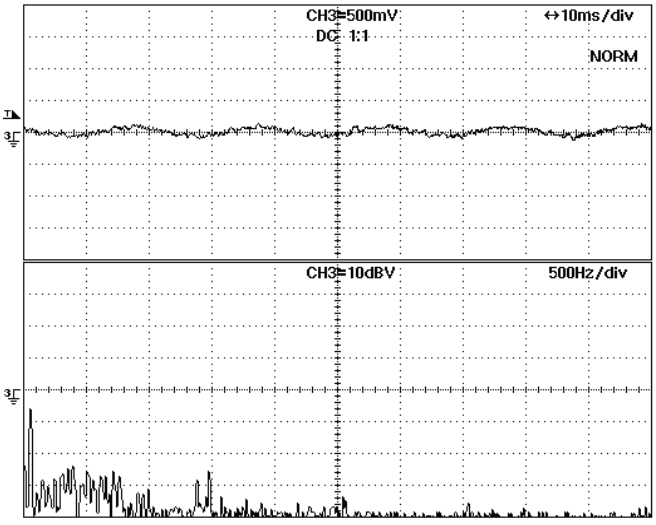

b)

Fig. 9. a) Power spectral density of line current (i_A). b) Power spectral density of input matrix current (i_b).

6. Conclusions

In this chapter, after a brief discussion about the use of static power converters for power conditioning and quality improvement within electric power networks, an application was proposed for a three-phase matrix converter based UPFC without energy storage, exploiting the ease of interaction of this converter with the electrical grid, and their benefits in replacing the classical topologies with associations of back-to-back converters. For this new UPFC topology, dynamic models of matrix converter based UPFC in *dq* coordinates were obtained. Despite its control complexity, matrix converters have advantages (weight, size and maintenance) and present good performance as power flow controllers in the electrical power grid in comparison to back-to-back converter topologies.

The solution here proposed uses inverse dynamics decoupled linear controllers based in control algorithms applied to a multivariable system, and have the ability to compensate the cross-terms existing in the control loop.

The controller design was validated using simulation and experiments. Results presented in this chapter show that active and reactive components of power flow can be advantageously controlled using the proposed matrix converter based UPFC.

The design of the inverse dynamics decoupled linear controllers is dependent on the transmission line parameters, the controllers being sensitive to the system parameters. Nevertheless, simulation and experimental results show that the active and reactive power controllers, as designed, exhibit almost no cross-coupling between active and reactive power and guarantee fast response, as well as very little sensitivity to system parameters.

7. References

Alesina A. and Venturini, M. G. B. "Solid-state power conversion: A Fourier analysis approach to generalized transformer synthesis" IEEE Trans. Circuits Systems, vol. CAS-28, pp. 319–330, Apr. 1981.

Galkin, I.; Ribickis, L.; "Control of Reactive Power by means of Matrix Converters"; Proc. EPE'01 Conf., Graz, Lausanne, Aug. 2001.

Gyugyi, L., "Unified Power Flow Control Concept for Flexible AC Transmission Systems" IEE PROCEEDINGS-C, vol. 139, No 4, Jul. 1992.

Hingorani N.; Gyugyi, L.; Understanding FACTS – Concepts and Technology of Flexible AC Transmission Systems, IEEE Press, A John Wiley &Sons Inc., Publication, 2000.

Huber L., Borojevic, D. and Burany N., "Analysis design and implementation of the space-vector modulator for forced-commutated cycloconvertors", IEE Proceedings-B Vol. 139 No.2, March 1992, pp 103-113.

Liu, L.; Zhu, P.; Kang, Y.; Chen, J.; "Power-Flow Control Performance Analysis of a Unified Power-Flow Controller in a Novel Control Scheme", IEEE Transactions on Power Delivery, vol. 22, No 3, pp. 1613-1619, July 2007.

Matsuo, T.; Bernet, S.; Colby, R. S.; Lipo, T.; "Modelling and Simulation of Matrix Converter/Induction Motor Drive"; Proc. ELECTRIMACS'96 Conf., pp. 1-10, Saint-Nazaire, France, Sep 1996.

Monteiro, J.; Silva, J.: Pinto, S.; Palma, J.; "Unified Power Flow Controllers without DC Bus: Designing Controllers for the Matrix Converter Solution", Proc. of the International Conference on Electrical Engineering (CEE'05), Coimbra, Portugal 2005.

Nikkhajoei H., Iravani, M. "A Matrix Converter Based Micro-Turbine Distributed Generation System", IEEE Trans. On Power Delivery, Vol. 20, No. 3, July 2005.

Pinto, S.; Silva, J.; "Sliding Mode Direct Control of Matrix Converters", IET Electric Power Applications, 1 (3), pp. 439-448, 2007.

Round, S. D.; Yu Q.; Norum, L. E.; Undeland, T. M.; "Performance of a unified power flow controller using a d-q control system". Conference Publication Ac and Dc Power Transmission, 1(423), 1996.

Song, Y.H. and Johns, A.T.; "Flexible AC Transmission Systems", IEE Power and Energy series, UK, 1999.

Verveckken, J.; Silva, F.; Driesen, J. "Design of Inverse Controller with Cross-Coupling Suppression for UPFC Series Converter" EUROCON 2007, The International Conference on "Computer as Tool" Warsaw, September 9-12.

Wang, B., Venkataramanan, G. "Dynamic Voltage Restorer Utilizing a Matrix Converter and Flywheel Energy Storage", IEEE Tran. on Industry Applications, Vol. 45, No 1, pp. 222– 231, Jan/Feb 2009.

Wheeler, P.; Rodriguez, J.; Clare, J.; Empringham, L.; Weinstein, A., "Matrix Converters: A Technology Review," IEEE Trans. Industrial Electronics, vol. 49, No 2, pp. 276–288, Apr. 2002.

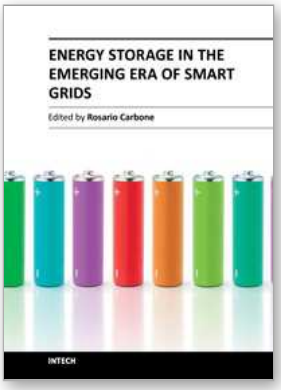

Energy Storage in the Emerging Era of Smart Grids

Edited by Prof. Rosario Carbone

ISBN 978-953-307-269-2
Hard cover, 478 pages
Publisher InTech
Published online 22, September, 2011
Published in print edition September, 2011

Reliable, high-efficient and cost-effective energy storage systems can undoubtedly play a crucial role for a large-scale integration on power systems of the emerging â€œdistributed generationâ€ (DG) and for enabling the starting and the consolidation of the new era of so called smart-grids. A non exhaustive list of benefits of the energy storage properly located on modern power systems with DG could be as follows: it can increase voltage control, frequency control and stability of power systems, it can reduce outages, it can allow the reduction of spinning reserves to meet peak power demands, it can reduce congestion on the transmission and distributions grids, it can release the stored energy when energy is most needed and expensive, it can improve power quality or service reliability for customers with high value processes or critical operations and so on. The main goal of the book is to give a date overview on: (I) basic and well proven energy storage systems, (II) recent advances on technologies for improving the effectiveness of energy storage devices, (III) practical applications of energy storage, in the emerging era of smart grids.

How to reference

In order to correctly reference this scholarly work, feel free to copy and paste the following:

Joaquim Monteiro, J. Fernando Silva, Sónia Pinto and João Palma (2011). Unified Power Flow Controllers Without Energy Storage: Designing Power Controllers for the Matrix Converter Solution, Energy Storage in the Emerging Era of Smart Grids, Prof. Rosario Carbone (Ed.), ISBN: 978-953-307-269-2, InTech, Available from: http://www.intechopen.com/books/energy-storage-in-the-emerging-era-of-smart-grids/unified-power-flow-controllers-without-energy-storage-designing-power-controllers-for-the-matrix-con

INTECH
open science | open minds

InTech Europe
University Campus STeP Ri
Slavka Krautzeka 83/A
51000 Rijeka, Croatia
Phone: +385 (51) 770 447
Fax: +385 (51) 686 166
www.intechopen.com

InTech China
Unit 405, Office Block, Hotel Equatorial Shanghai
No.65, Yan An Road (West), Shanghai, 200040, China
中国上海市延安西路65号上海国际贵都大饭店办公楼405单元
Phone: +86-21-62489820
Fax: +86-21-62489821